

Distance of the Seyfert 2 galaxy IC2560 and the Hubble constant

Naomasa Nakai¹ , Aya Yamauchi², Madoka Yamazaki³
and Reo Harada¹

¹Kwansei Gakuin University, Sanda-shi, Hyogo 669-1330, Japan. email: ilo77771@kwansei.ac.jp

²National Astronomical Observatory of Japan, Oshu-shi, Iwate 023-0861, Japan

³University of Tsukuba, Tsukuba-shi, Ibaraki 305-8571, Japan

Abstract. Water vapor maser emission from a Seyfert 2 galaxy IC2560 was observed with sensitive VLBI. The accurate black hole mass was determined by separating the mass of the disk surrounding the black hole. In addition, the distance of the galaxy was directly measured from the maser disk. The Hubble constant determined using the distances and recession velocities of IC2560 and other megamasers is inconsistent with that determined with CMB by $3\text{--}6 \text{ km s}^{-1} \text{ Mpc}^{-1}$.

Keywords. Active galactic nuclei, Angular diameter distance, Hubble constant, Water vapor maser

1. Introduction

IC 2560 is a SBb galaxy located at the distance of 44 Mpc. Its nucleus is classified as a Seyfert 2. Braatz *et al.* (1996) detected water vapor maser emission at the systemic velocity of the galaxy, Ishihara *et al.* (2001) detected blue- and red-shifted high-velocity features (Figure 1) and made VLBI observations of the systemic velocity features, and Yamauchi *et al.* (2012) made VLBI observations of the systemic features and a part of red-shifted features. In addition, Yamauchi *et al.* (2012) detected the velocity drift of the systemic features.

We made new sensitive VLBI observations of both the systemic velocity features and all blue- and red-shifted high-velocity features in 2010, using VLBA and GBT. The synthesized beam was about $1.5 \times 0.35 \text{ mas}$. Here we show results of the observations with VLBI, determine the distance of the galaxy and estimate the Hubble constant. Details of the results will be presented by Yamauchi *et al.* (in preparation).

2. Maser distribution and rotation curve

Figure 2a shows the distribution of the maser spots on the sky which exhibits an edge-on maser disk. Figure 2b is the velocity of the maser spots along the disk. By fitting the velocity distribution with the power law of the rotation curve profile, α , the systemic velocity V_{sys} and the center position of the galaxy were determined. Figure 2c is the resultant rotation curve of the maser spots. If we fit the rotation curve with $V_{\text{rot}} \propto r^\alpha$, the power is $\alpha = -0.415 \pm 0.022$. If $|\alpha| = 0.5$, the rotation is Keplerian, i.e., only point mass exists at the center. The lower power of $|\alpha| < 0.5$ however indicates non-negligible mass distribution around the central mass. Thus we adopt two mass components model of the central mass and disk mass rotating around the center showed in Figure 3. In

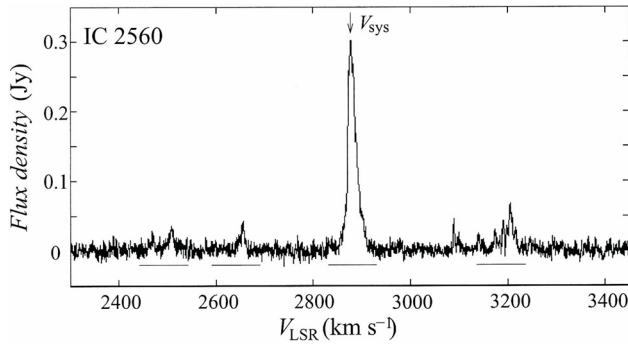


Figure 1. Maser spectrum of IC2560.

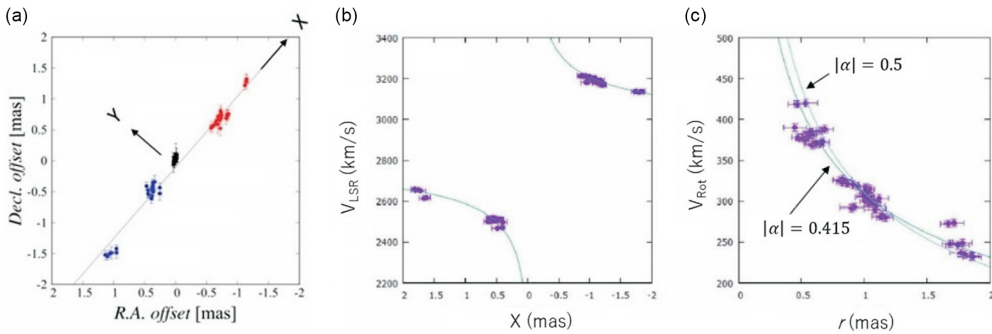


Figure 2. (a) Distribution of maser spots on the sky. (b) Velocities along the maser disk. (c) Rotation curve of the maser disk.

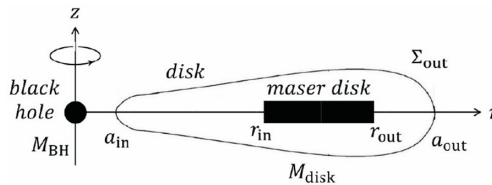


Figure 3. Schematic view of the central black hole and the gas disk rotating around the black hole.

this case, the centripetal force gives the equation,

$$\frac{V_{\text{rot}}^2}{r} = G \frac{M_{\text{BH}}}{r^2} + \frac{\partial \Psi_{\text{disk}}}{\partial r} \tag{1}$$

where M_{BH} is the central mass (i.e., black hole mass) and Ψ_{disk} the potential of the disk at r . We follow the mass model of the disk by Hure (2002), Hure & Hersant (2007) and Hure *et al.* (2008), adopting the distribution of the surface density in the disk,

$$\Sigma_{\text{disk}}(r) = \Sigma_{\text{out}} \left(\frac{r}{a_{\text{out}}} \right)^\beta \tag{2}$$

Adopting the Mestel disk ($\beta = -1$) and assuming $a_{\text{in}} \ll a_{\text{out}}$ and $r_{\text{out}} \ll a_{\text{out}}$,

$$\frac{\partial \Psi_{\text{disk}}}{\partial r} = 2\pi G \Sigma_{\text{out}} \frac{a_{\text{out}}}{r} \tag{3}$$

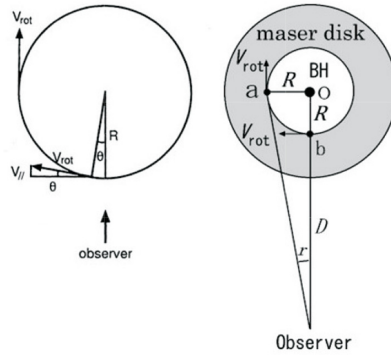


Figure 4. Geometry of the maser disk.

Equations (1) and (2) gives

$$V_{\text{rot}} = \sqrt{\frac{GM_{\text{BH}}}{r} + 2\pi G\Sigma_{\text{out}}a_{\text{out}}}. \tag{4}$$

Fitting the rotation curve (Figure 2c) with equation (4),

$$M_{\text{BH}} = (4.14 \pm 0.17) \times 10^6 [M_{\odot}]. \tag{5}$$

The disk mass within the outer edge of the maser disk is given by

$$M_{\text{disk}} = \int_{a_{\text{in}}}^{r_{\text{out}}} \Sigma_{\text{disk}}(r)2\pi r dr = 2\pi\Sigma_{\text{out}}a_{\text{out}}(r_{\text{out}} - a_{\text{in}}) = (1.67 \pm 0.27) \times 10^6 [M_{\odot}], \tag{6}$$

which is 40 % of the black hole mass.

3. Distance of IC2560

The linear radius of the maser disk is determined by

$$R = V_{\text{rot}}^2/\alpha, \tag{7}$$

using the acceleration of the systemic features, $\alpha = dV_{||}/dt = 2.593 \pm 0.027 \text{ km s}^{-1} \text{ yr}^{-1}$ measured by Yamauchi *et al.* (2012) (Figure 4). The apparent radius, r , is directly determined by the rotation curve and the systemic features, as shown in Figure 5. Then the distance to the galaxy is determined to be $D = R/r = 44.5 \pm 6.1 \text{ Mpc}$.

4. Hubble constant

The flat universe model ($K = 0, \Omega_m + \Omega_\lambda = 1$) gives the angular-size distance,

$$D_A \cong \frac{cz}{H_0} \left(1 - \left(2 + \frac{3}{2}\Omega_m \right) \frac{z}{2} \right), \tag{8}$$

where K is the curvature of the universe, $\Omega_m = 0.315$ the matter density parameter and Ω_λ the dark energy density parameter. The velocity of IC2560 is $cz = 3160.0 \pm 4.7 \text{ km s}^{-1}$, corrected the proper motion of our Galaxy to CMB. Figure 6 is the Hubble diagram of Pesce *et al.* (2020) adding IC2560 but removing NGC 4258 which is too close. Least square fitting gives the Hubble constant of $H_0 = 72.8 \pm 2.5 \text{ km s}^{-1} \text{ Mpc}^{-1}$ which is different from the values obtained from observations of CMB, $H_0 = 69.32 \pm 0.80 \text{ km s}^{-1} \text{ Mpc}^{-1}$ by Bennett *et al.* (2013) and $H_0 = 67.4 \pm 0.5 \text{ km s}^{-1} \text{ Mpc}^{-1}$ by Planck collaboration (2020), confirming Hubble tension.

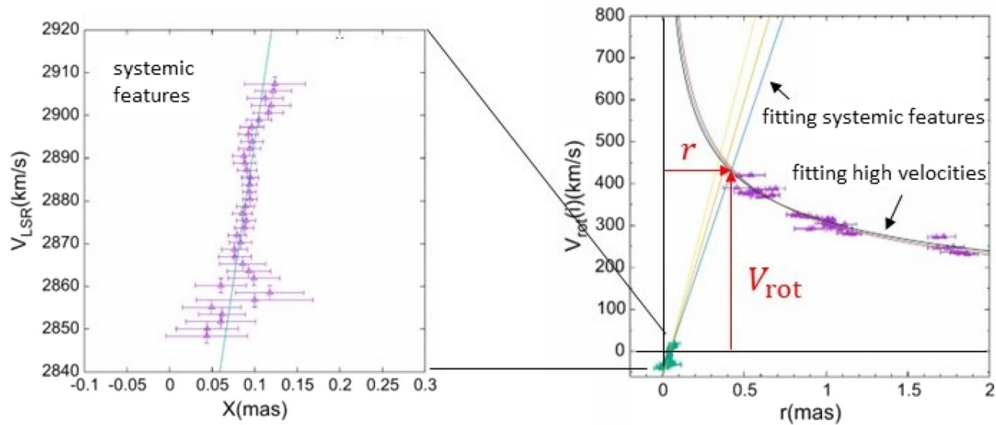


Figure 5. Velocities of the systemic and high-velocity features as a function of the distance from the center.

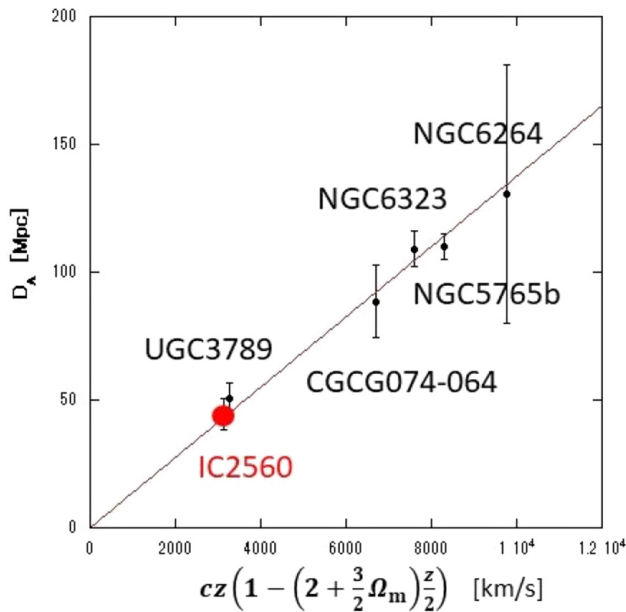


Figure 6. Relation between the recession velocity and the distance of megamasers.

References

- Bennett, C. L., *et al.* 2013, *ApJS*, 208, 20
 Braatz, J. A., Wilson, A. S., & Henkel, C., 1996, *ApJS*, 106, 51
 Hure, J.-M., 2002, *A&A*, 395, L21
 Hure, J.-M., & Hersant, F. 2007, *A&A*, 467, 907
 Hure, J.-M., Hersant, F., Carreau, C., & Busset, J.-P. 2008, *A&A*, 490, 477
 Ishihara, Y., Nakai, N., Iyomoto, N., Makishima, K., Diamond, P., & Hall, P. 2001, *PASJ*, 53, 215
 Pesce, D. W., *et al.* 2020, *ApJ*, 891, L1
 Planck collaboration., 2020, *A&A*, 641, A6
 Yamauchi, A., Nakai, N., Ishihara, Y., Diamond, P., & Sato, N. 2001, *PASJ*, 64, 103